

FREE CONVECTIVE HEAT TRANSFER FOR A TILTED ELECTRONIC ASSEMBLY EQUIPPED WITH QFN64 DEVICE

Bairi A.

University of Paris
Laboratoire Thermique Interfaces Environnement,
LTIE-GTE EA 4415
50, rue de Sèvres, F-92410 Ville d'Avray
France
E-mail: abairi@u-paris10.fr, bairi.a@gmail.com

ABSTRACT

The Quad Flat No-lead 64 type device (QFN64) is increasingly used in electronics giving its well known advantages. Its correct operation is nevertheless associated to adequate thermoregulation in accordance with the manufacturers' recommendations. The printed circuit board (PCB) containing this active component is installed in cavities with different form and dimensions according to the intended application. The heat transfer by natural convection phenomenon with air is often favoured in applications. The thermal design of these electronic assemblies then requires the full control of the natural convective heat transfer exchanges that occur on all the assembly's areas. It does not exist in the specialized literature correlations to determine accurately the convective heat transfer coefficients concerning the treated QFN64 whose high generated volumetric power can reach several GWm^{-3} . The objective of the present work is to characterize the natural thermal phenomena concerning these arrangements and quantify through easy to use correlations these convective heat transfer coefficients according to the power generated by the QFN64 and the inclination angle of the PCB with respect to the horizontal. These data are useful for the thermal control and design of this interesting electronic assembly. The work is based on a 3D numerical approach by means of the control volume method.

NOMENCLATURE

a	$[\text{m}^2\text{s}^{-1}]$	thermal diffusivity
C_p	$[\text{J kg}^{-1}\text{K}^{-1}]$	specific heat at constant pressure
g	$[\text{m.s}^{-2}]$	acceleration of the gravity
h_i	$[\text{Wm}^{-2}\text{K}^{-1}]$	local free convective heat transfer coefficient
\bar{h}	$[\text{Wm}^{-2}\text{K}^{-1}]$	average free convective heat transfer coefficient
\bar{h}_Q	$[\text{Wm}^{-2}\text{K}^{-1}]$	QFN's global free convective heat transfer coefficient
\bar{h}_B	$[\text{Wm}^{-2}\text{K}^{-1}]$	PCB's global free convective heat transfer coefficient
L	$[\text{m}]$	characteristic length
m	$[-]$	number of elements

P	$[\text{W}]$	generated power
p	$[\text{Pa}]$	pressure
p^*	$[-]$	dimensionless pressure
Pr	$[-]$	Prandtl Number
Ra	$[-]$	Rayleigh Number
S_i	$[\text{m}^2]$	area of the i th element
S_h	$[\text{m}^2]$	external area
T	$[\text{K}]$	temperature
T^*	$[-]$	dimensionless temperature
T_i	$[\text{K}]$	local temperature

Greek symbols

α	$[\text{°}]$	PCB's inclination angle with respect to the horizontal
β	$[\text{K}^{-1}]$	volumetric expansion coefficient
$\bar{\nabla}^*$	$[-]$	dimensionless Nabla Operator
∇^{*2}	$[-]$	dimensionless Laplacian
μ	Pa.s	kinematic viscosity
ϕ	$[\text{Wm}^{-3}]$	volumetric heat flux

INTRODUCTION

Thermoregulation of the electronic assemblies is essential for their correct operation and requires a special study for each application. The increasing miniaturization of the active electronic devices poses important thermal problems. Given their very low volume and operating power, the QFN packages generate very high volumetric heat fluxes which can reach several GWm^{-3} . This is the case of the Quad Flat No Lead 64 (denoted here QFN64) examined in the present work. This device is nowadays one of the most used components in the electronic assemblies and it concerns various engineering areas. This low cost and easy implementation component has interesting thermal and electrical performances. Its small size and weight allow its installation into low volume devices, as for example for notebook computers. It is also used in several daily life devices as in the portable cell phones and other household appliances (washing machine, dishwasher, air conditioner, boiler ...). Its electrical performance allows its integration in the many assemblies associated with high power and frequency. Its

thermal characteristics make it competitive with respect to other conventional devices and evolution of its manufacturing techniques makes it more reliable. Many works are done to improve the QFN64's performance, given the perspectives for its generalization in the assemblies. Many of them are devoted to the heat transfer phenomena as the thermal control of this component during operation is essential. Its technical characteristics widely available in the literature can be found in the technical note [1]. Additional information and the most widely used standards for thermal tests are contained in specialized technical notes such as [2,3]. The weak point of the QFN is its low reliability when it is subjected to many heat cycles, which is the case for some applications. These solicitations cause often failures resulting to deactivation of the electronic assembly. In some cases, the QFN can not be used because the thermal phenomena lead to its destruction. This is due in part to the very different values of the thermal expansion coefficients of the materials that constitute the QFN and those of the printed circuit boards (PCB) on which they are welded, as confirmed by the study [4]. The opportunity of QFN implementation thus requires prior study with real thermal cycles to control their reliability in dynamic mode. The work [5] provides a technique for predicting fatigue and durability of these components when they are subjected to thermal cycling. Tests were carried out by varying many physical parameters to include different possibilities of actual operation. The thermal cycles are performed on several QFN types. The tests are done in a temperature range varying between -40°C and $+150^{\circ}\text{C}$, covering the extreme operative conditions of these electronic components. Some QFN manufacturing steps also induce thermal problems related to thermo-mechanical properties of the electronic assembly's materials (thermal stresses, maximum permissible temperature, thermal expansion, ...). The special case of the component's deformation during its manufacture is numerically examined in [6] by means of the finite element method. Excessive temperature at the junctions and contact between the components and the printed circuit board may cause assembly's malfunctions. This known phenomenon was confirmed in the study [7] devoted to the power amplifiers used in the radio frequency field. The study shows that exceeding the maximum temperature at junctions significantly reduces the reliability of the assembly. The correct sizing of electronic assemblies using localized heat sources of the QFN type requires exact knowledge of the heat exchanges that occur with the environment. When thermoregulation of these assemblies is made by natural convection as it is often the case in applications, engineers must be able to determine the average natural convective heat transfer coefficient corresponding to each surface of the QFN and the printed circuit board on which it is welded. This is the objective of the present study in which correlations are proposed, allowing to calculate the overall convective exchange coefficient for the QFN64 device and the PCB, according to the power generated by the component and the PCB's inclination angle relative to the horizontal plane. They concern several configurations obtained by varying the tilt angle between 0° (horizontal position) and 90° (vertical position) and the generated power in the range 10-100mW.

THE STUDIED CASE. SOLUTION

The assembly considered in this work is shown in Fig. 1. It consists of a square printed circuit board (PCB epoxy-copper 100mm x 100mm, Fig. 1 (a)) on which is welded the QFN64 (Fig. 1 (a) detailed in Fig. 1 (b-c)), randomly positioned. The position of device does not influence or only marginally the average convective heat transfer coefficients as has been shown in [8-10] for the QFN16 and 32.

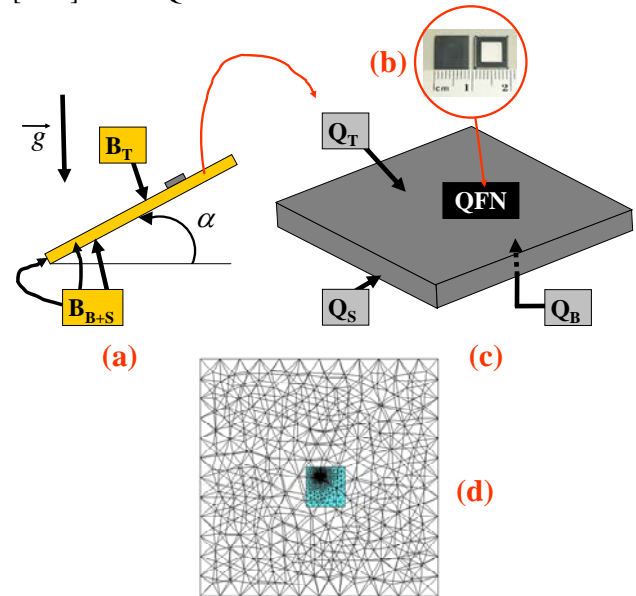


Figure 1. The considered assembly (a) the inclined PCB with QFN64 (b) - (c) details of the QFN64 and the exchange areas (d) the mesh QFN64-PCB-fluid volume

The assembly is disposed in a cubic air-filled closed cavity whose dimensions (700mm x 700 mm) are sufficiently large compared with those of the board, in order to not disturb the natural convective flow around the PCB and the QFN. Additional calculations were made assuming smaller plate and cavity that concern small-volume assemblies (case of the cell phone). The results show that the dimensions affect the dynamic phenomena of the flow but they affect only marginally the values of the average convective heat transfer coefficients, the main objective of the present survey. This is mainly due to the low generated power considered in this survey. The whole calculating domain including air is assumed initially isothermal at the minimum temperature ($T_c = 20^{\circ}\text{C}$). We shall not detail in this work the composition of the QFN and its different models used in applications. The reader can find all the characteristics of this component in the literature mentioned in the introduction. The recent works [8-10] examine the natural convection for assemblies equipped with QFN16 and 32 which are used for special applications that are different from those of the QFN64. The source of this device generates during operation a constant heat flux density $\phi = P/V$, where V and P are the volume of the source and its actual generated power, which varies between 0.01 (standby component, off) and 0.1W. The PCB may be inclined relative to the horizontal by an angle

α varying between 0° (horizontal PCB) and 90° (vertical) depending on the application.

The natural convective phenomena are examined all around the assembly which is decomposed into four distinct surfaces detailed Fig. 1: (i) the top of the QFN denoted as (Q_T) ; (ii) the four lateral faces of the QFN denoted as (Q_S) ; (iii) the entire rear face of the PCB and its four lateral surfaces, denoted as (B_{B+S}) ; (iv) the PCB's top face minus the back surface of the QFN64, denoted as (B_T) . The QFN's materials are assumed as isotropic for the pure heat conductive phenomena. Their thermal conductivities are furthermore assumed as temperature independent in the thermal range concerned by this study. This is not the case for the PCB since it consists of a substrate (epoxy) and copper whose thermal conductivities are very different. The equivalent conductivity in PCB's plane is thus different from that of its thickness. The same conductivities used in [8-10] are considered in this work. The heat exchange surface S_h is composed of m elements which exchange surface and temperature are denoted as S_i and T_i ($i=1,m$) respectively. Initially, the fluid and the whole assembly are isothermal at temperature T_c . Calculations are done by imposing a constant volumetric heat flux ϕ to the active part of the Die. The no-slip condition is assumed on the QFN package and on the PCB board. The environment temperature is kept constant at T_c , thermophysical properties are systematically evaluated at the average temperature of each control volume and the Boussinesq approximation is applied. In this numerical approach, the radiative heat transfer is not considered. This condition is realized by imposing a global infrared emissivity equal to zero at all walls. This simplifies the calculation process by considering only the convective exchange surface, which is the objective of this work. Some calculations have nevertheless been carried out by varying the surface emissivities. The results show that in the extreme case, the radiation is of about 3% of the global surfacic heat transfer, considering the low surface temperatures of the assembly and its dimensions. Calculations are done by means of the commercial software Ansys-Fluent [11] based on the control volume method and using the SIMPLE algorithm. Several configurations were also calculated with a CFD house code to check the previous calculations. The deviation is systematically less than 2% with regard to the convective heat transfer, the main objective of this study. Distribution of the surface temperature and temperature gradient of the overall m elements of the assembly (QFN package and PCB board) are processed with a specific home code developed in the LTIE in order to determine the local convective heat transfer coefficient

$$h_i = -\lambda(\partial T / \partial n) / (T - T_c)_i ; (i = 1, m); \quad (1)$$

whose integration weighted with the corresponding surfaces S_i over the total surface allows determination of the average

convective heat transfer coefficient $\bar{h} = \left(\sum_i h_i S_i \right) / \sum_i S_i$ corresponding to the considered area for a specific (P, α) combination. The global heat transfer coefficients \bar{h}_Q and \bar{h}_B corresponding to the QFN64 and the PCB respectively are then calculated by weighting the \bar{h} values over the corresponding areas. The mesh is constituted by quadrilateral wall faces and a combination of tetrahedral, hexahedral and pyramidal cells. A refinement is done in the wall region for the accurate determination of thermal gradients. The numerical solution is considered as mesh independent when the variation of successive \bar{h} values are less than 3% after 2% of mesh-refining. The adopted convergence criteria are set to 10^{-5} for the velocity components and 10^{-6} for the energy. Such conditions are attained with 522,487 cells and heat balance is done to control the calculation convergence. Some measurements of the power generated by the electronic device and temperature difference $(T - T_c)$ by means of K type thermocouples helped to validate the main results obtained with this numerical approach. The deviations experience-calculation are low, of around 3% on average being the maximum of 4% observed for the most unfavorable case. The experimental part is not detailed in this short paper devoted to the numerical study.

RESULTS

Many configurations have been considered by combining (i) the PCB board's inclination angle α between 0° and 90° by steps of 30° ; (ii) the generated power varying between 0.01W and 0.1W by steps of 0.01W. The streamlines corresponding to the horizontal and vertical positions as well as the dimensionless temperature for the horizontal position are presented in Fig. 2 for the maximal power $P = 0.1W$. When the assembly is horizontal, the heat flow bypasses the board PCB. The fluid is almost stagnant over (B_{B+S}) and over a large part of its upper free surface. A flow nevertheless occurs on the upper face of the package towards its vertical. It starts in the area where the streamlines converge and this area remains continuous while decreasing towards the upper part of the enclosure. This flow is relatively distant from the electronic component areas (Q_T) and (Q_S) . Almost entire surface (B_{B+S}) is isothermal, near T_c value. Only the area around the upper side of the device is heated by conduction through the legs. The heat is drained towards the upper copper layer of the plate, thus ensuring a better cooling of the component. The heating reaches only weakly the side surfaces of the PCB and the temperature of the bottom corners of the component are near the minimum temperature T_c .

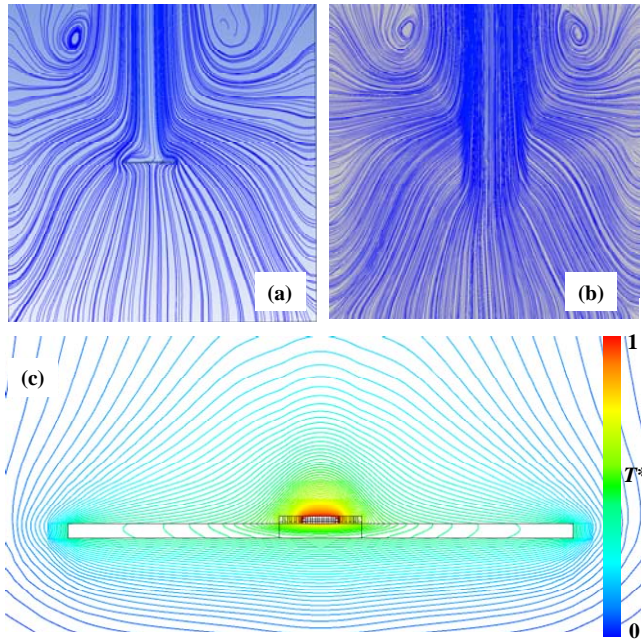


Figure 2. Streamlines for $P = 0.1W$ corresponding to (a) the horizontal position (b) the vertical position of the PCB (c) dimensionless temperature for the horizontal position

The isotherms almost parallel in the fluid show a temperature stratification slightly deformed by the natural convective flow in the area above the component. These observations remain valid regardless of the position of the QFN on the PCB. When the PCB is vertical, the convective flow is concentrated in the vicinity of the component. The average velocity in this area increases as the power generated increases, and the flow is accelerated as the air rises the plate. The air stagnates at the bottom edge of the plate. Boundary layer phenomena which develop on the vertical wall improves the convective heat exchange but not significantly with respect to the horizontal position. The maximum temperature always reached in the center is still lower for the vertical position, which is due to the dynamic phenomena described above. The temperature distribution on the upper face of the component (Q_T) does not undergo substantial change compared with that of the horizontal position. Only the absolute value of the temperature is different in both configurations, being weaker in the vertical position. The PCB inclination angle α affects the flow around the component and its thermal state. The obstacle of the lower face of (Q_S) becomes less sensitive as the slope increases.

The distribution of local convective heat transfer coefficient and the average values \bar{h} were determined for all combinations (P, α) and on every surface. The results are shown Fig. 3(a) for (Q_T) and (Q_S) (QFN areas) and in Fig. 3(b) for (B_T) and (B_{B+S}) (PCB areas). In the vertical position, the \bar{h} values are different on the four faces of (Q_S), in accordance with the

dynamic aspects described above. The maximum and minimum \bar{h} values correspond to the lower and upper side of (Q_S) respectively, and the intermediate value is located on the two lateral faces, with a slight predominance for its face nearest to the PCB edge. The average heat exchange on these two (Q_S) side faces is close to that of the upper face (Q_T) for this vertical position while it is almost the same on the four lateral faces for the horizontal position. The average heat exchange on the two united surfaces together (Q_T) + (Q_S) is more important for the vertical position and it increases for both cases when the generated power increases. For all the treated inclinations, the convective heat transfer on the PCB is concentrated on its upper free side around the package, which is heated by conduction through the legs of the component.

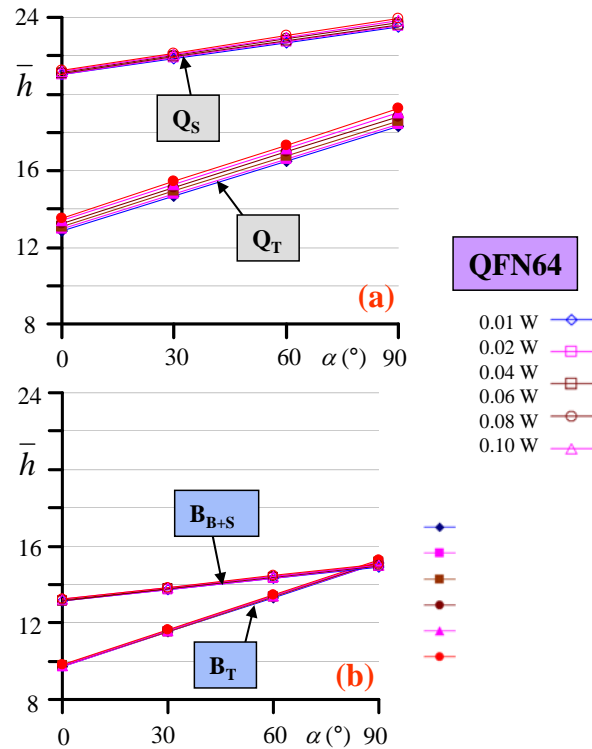


Figure 3. Evolution of the average convective heat transfer coefficient \bar{h} (a) on (Q_T) and (Q_S); (b) on (B_T) and (B_{B+S})

The results for the considered power and inclination angle ranges lead to the following correlations

$$\begin{cases} \bar{h}_Q = 12.8 + 0.06\alpha + (7.4 + 0.034\alpha)P \\ \bar{h}_B = 11.5 + 0.04\alpha + (1.3 + 0.004\alpha)P \end{cases} \quad (2)$$

Valid for $\begin{cases} \text{QFN64} \\ 0 \leq \alpha \leq 90^\circ \\ 0.01 \leq P \leq 0.1W \end{cases}$

They allow determination of the overall natural convective heat transfer coefficients \bar{h}_Q and \bar{h}_B corresponding to the QFN and the PCB exchange areas respectively, according to the generated power P and the inclination angle α of the PCB. The evolution of these coefficients is presented in Fig. 4(a)-(b) versus P and α respectively.

CONCLUSION

The aerothermal phenomena concerning an electronic assembly equipped with a QFN64 active device have been qualified in this work. Natural convective heat transfer exchanges are quantified for this component and the printed circuit board on which it is welded. The proposed correlations allow determination of the overall natural convective heat transfer coefficients on the QFN and the PCB exchange areas respectively, according to the generated power P and the inclination angle α of the PCB. They are valid for all configurations obtained by varying the PCB's tilt angle between 0° (horizontal position) and 90° (vertical position) and the QFN64's generated power between 10 and 100mW. These angle and power ranges correspond to particular onboard electronics applications, but they can be used for the thermal design of this electronic assembly in various engineering fields.

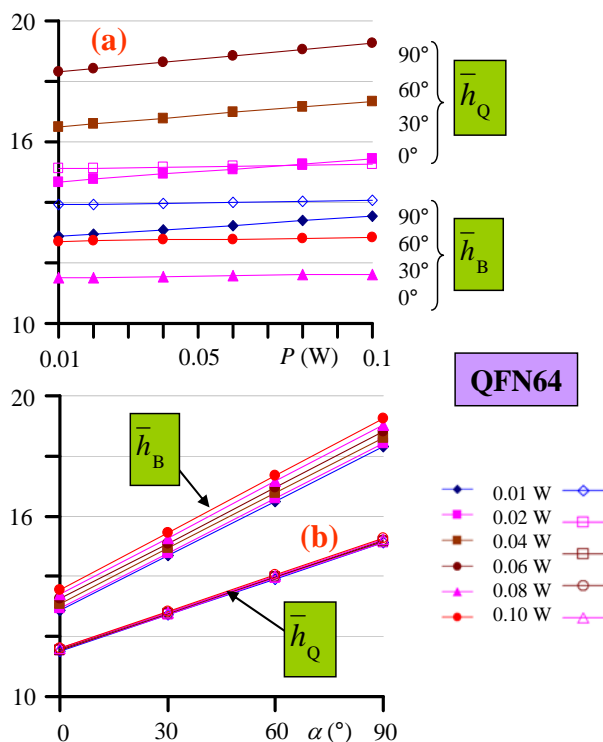


Figure 4. Evolution of the overall natural convective heat transfer coefficients \bar{h}_Q for the QFN64 and \bar{h}_B for the PCB

(a) versus P ; (b) versus α .

REFERENCES

- [1] Trinamic application note 005, Rev. 1.01, <http://www.trinamic.com>, 2013.
- [2] Integrated Circuits Thermal Test Method Environmental Conditions - Natural Convection (Still Air), Jedec Solid State Technology Association, JESD51-2A, 2008.
- [3] Guidelines for Reporting and Using Electronic Package Thermal Information, Jedec Solid State Technology Association, JESD51-12, 2005.
- [4] J. de Vries, M. Jansen, W. Van Driel, Solder-joint reliability of HVQFN-packages subjected to thermal cycling, *Microelectronics Reliability* 49 (2009) 331–339.
- [5] T.Y. Tee, H.S. Ng, D. Yap, Z. Zhong, Comprehensive board-level solder joint reliability modeling and testing of QFN and power QFN packages, *Microelectronics Reliability* 43 (2003) 1329–1338.
- [6] D.G. Yang, K.M.B. Jansen, L.J. Ernst, G.Q. Zhang, W.D. van Driel, H.J.L. Bressers, J.H.J. Janssen, Numerical modeling of warpage induced in QFN array molding process, *Microelectronics Reliability* 47 (2007) 310–318.
- [7] Z. Radivojevic, K. Andersson, J.A. Bielen, P.J. Van der Wel, J. Rantala, Operating limits for RF power amplifiers at high junction temperatures, *Microelectron. Reliab.* 44 (2004) 963–972.
- [8] A. Baïri, Thermal design of tilted electronic assembly with active QFN16 package subjected to natural convection, *International Communications in Heat and Mass Transfer* 66 (2015) 240–245.
- [9] A. Baïri, Natural convection on inclined QFN32 electronic package generating constant volumetric heat flux, *International Communications in Heat and Mass Transfer* 66 (2015) 133–139.
- [10] A. Baïri, O. Haddad, Detailed correlations on natural convective heat transfer coefficients for QFN32 electronic device on inclined PCB, *Numerical Heat Transfer, Part A: Applications*, (2016), DOI 10.1080/10407782.2015.1090850.
- [11] Fluent-Ansys, Elements Reference, Release 13.0 (2010), Swanson Analysis Systems, Inc.